Effect of the image potential on excitons in semi-infinite semiconductors

D. Viri and R. Del Sole
Istituto Nazionale di Fisica della Materia, Dipartimento di Fisica, Università di Roma "Tor Vergata," via della Ricerca Scientifica 1, 00133 Roma, Italy
(Received 26 May 1995)

The effect of the image potential on Wannier-exciton wave functions is studied perturbatively within the effective-mass approximation. We show that the image potential increases the dead- and transition-layer depths by about 10%. These differences lead to small changes in the optical spectra.

I. INTRODUCTION

The determination of exciton wave functions near a surface is a difficult quantum-mechanical problem. Even modeling the surface as an infinite potential barrier, the very fact that the electron and the hole interact separately with the surface induces a coupling between the relative and center-of-mass motions.[1] As a result, an exciton undergoes a deformation when scattering against the surface and an exciton-free layer, where the probability of finding an exciton is strongly reduced, occurs below the surface.[2] The details of the wave function near the surface are important in determining the reflection coefficient of light. Moreover, since they establish the relative amplitudes of the two propagating waves (lower and upper polaritons), they also determine the transmission coefficient. The depth of the exciton-free layer, or dead layer, has been a matter of debate for many years, with estimates, based either on theory or experiment, ranging from 0.5 to 2 exciton radii.[3]

Understanding the exciton motion near a surface has required several years of work. Most solutions of the problem rely on the adiabatic separation of the center-of-mass slow motion along z (perpendicular to the surface) from the relative electron-hole (e-h) fast motion.[4–7] In order to provide a good estimate of the dead layer, high accuracy is required in the solution of the relative e-h motion,[7] which is obtained by extending Satpathy's exact solution[8] of the surface impurity problem to the case of an exciton with fixed center of mass. Then the center-of-mass wave function is found by numerical one-dimensional integration. The adiabatic separation is valid for small e-h mass ratio m_e/m_h; for values of this ratio of the order of unity, an alternative numerical solution, not involving the adiabatic approximation, has been given by D'Andrea and Del Sole.[1,7] (For numerical reasons, this method does not work well for $m_e/m_h \ll 1$.) The two methods yield identical results for $m_e/m_h = 0.3$,[7] corresponding to the A exciton in CdS. Therefore it is possible, using the two methods in the respective ranges of validity, to determine exciton wave functions in the whole range of m_e/m_h. The picture coming out involves the simultaneous presence of a dead layer below the surface, where the exciton is now allowed at all, and of a transition layer below it, where the probability of finding the exciton grows continuously from zero up to the bulk value.[9] The thickness of the dead layer d and that of the transition layer $1/P$ depends on the ratio m_e/m_h: their sum ranges from $1.7a_B$ for $m_e/m_h \ll 1$ to $0.6a_B$ for $m_e/m_h = 1$ (a_B is the effective Bohr radius). This result, obtained only recently,[9] reconciles the different determinations of the dead-layer depth for different materials with one another, and all of them with theory. Reflectance spectra calculated from the wave functions discussed above are in satisfactory—good in some cases—agreement with experiments, with slight discrepancies occurring in a few cases.

The image potential, arising from the mismatch between the semiconductor dielectric constant ϵ and that of a vacuum, is ignored in the treatment described above. It is given by

$$V_{\mathrm{Im}}(\vec{\rho}_e-\vec{\rho}_h,z_e;z_h)=\frac{e^2}{\epsilon}\frac{\epsilon-1}{\epsilon+1}\times\left[-\frac{1}{\sqrt{(\vec{\rho}_e-\vec{\rho}_h)^2+(z_e+z_h)^2}}+\frac{1}{4z_e}+\frac{1}{4z_h}\right], \tag{1}$$

where $\vec{\rho}$ is the position in the surface plane, and subscripts e and h refer to the electron and to the hole, respectively. The first term in the square brackets is the attractive interaction of the electron with the image hole, while the second and third terms are the interaction of the electron with its image, and that of the hole with its image, respectively. The last two terms dominate very near the surface, where the image potential is strongly repulsive. However, the exciton wave function is very small there, due to the occurrence of the dead and transition layers, which are a consequence of the no-escape boundary condition.[1] As soon as the distance from the surface becomes larger than the exciton radius, the image potential becomes smaller and smaller, because the exciton is seen from the surface as a neutral point particle. Estimates of the image potential for some relevant cases, reported in Ref. 1, confirm that its effect might be small and are the rationale for neglecting it. This is quite different from the situation found in quantum wells, where the image potential yields relevant effects on the

binding energy.[10] The difference of course arises from the absence of confinement in the semi-infinite crystal: differently from the case of confined systems, the exciton, repelled from the surface by the adiabatic potential due to the no-escape boundary condition, cannot be found near the surface, where the image potential is important.

However, the slight discrepancies between calculated (ignoring the image potential) and measured reflectance spectra found for GaAs and InP, where the dead layer of the heavy-mass exciton is quite large,[9] suggest that an increase—although small—of the dead-layer depth, due to the image potential, might be responsible for them. The purpose of the present work is to check this possibility.

We will solve the exciton effective-mass equation within the adiabatic approximation by treating the image potential perturbatively. We will show that the image potential increases the dead- and transition-layer depths by about 10% with respect to the previous calculation. Its effect, however, is quite small in the calculated reflectance spectra. We conclude therefore that it is correct to neglect the image potential in semi-infinite semiconductors and that the residual, small discrepancies between theory and experiment in GaAS and—yet smaller—in InP must have a different origin.

The plane of the paper is as follows: In Sec. II we will extend Satpathy's treatment of a near-surface impurity to include perturbatively the image potential. In Sec. III the exciton center-of-mass motion will be considered and the dead- and transition-layer depths as a function of m_e/m_h will be calculated. In Sec. IV we will show the effect of the image potential on reflectance and will draw the conclusions of this work.

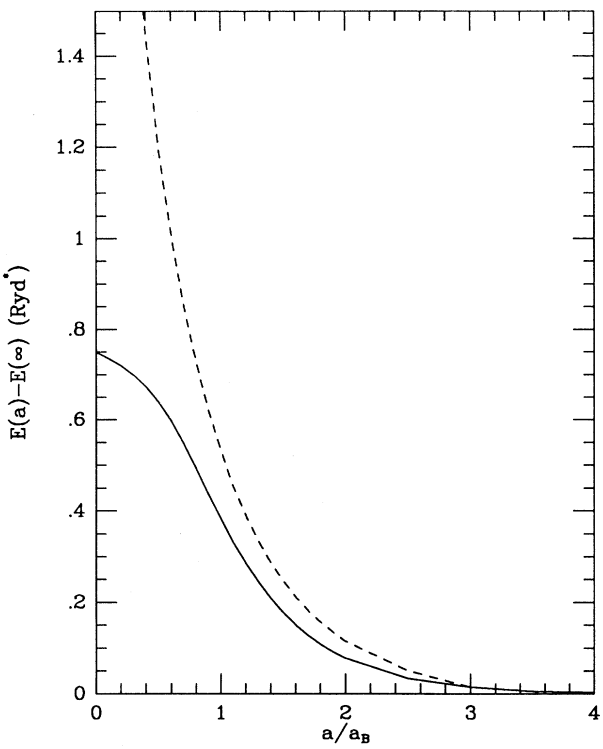

FIG. 1. Shift of the ground-state energy of a hydrogenic impurity with respect to the bulk value as a function of the distance a from the surface. Solid line: Satpathy's calculation (Ref. 8), not including image-potential effects. Dashed line: image potential included according to first-order perturbation theory, with $\epsilon=12.6$.

II. SURFACE IMPURITY

In this section we consider the effective-mass Schrödinger equation for an hydrogenic impurity at distance a from the surface:

$$\left[-\frac{\hbar^2}{2m_e}\nabla_e^2-\frac{e^2}{\epsilon\sqrt{\rho_e^2+(z_e-a)^2}}+V_{\mathrm{Im}}(\vec{\rho}_e,z_e;a)\right]\times\Psi(\vec{\rho}_e,z_e;a)=E(a)\Psi(\vec{\rho}_e,z_e;a)\ , \quad (2)$$

with the "no-escape" boundary conditions at the surface, located at $z=0$ (the semiconductor occupies the half-space $z\geq 0$):

$$\Psi(\vec{\rho}_e,0;a)=0\ . \quad (3)$$

Here $\vec{r}_e$ and m_e are the electron position and mass, respectively. Satpathy[8] has given the exact solution of this equation in the absence of the image potential, by showing that it is separable in parabolic coordinates, $\xi=(r_1+r_2)/2a$ and $\eta=(r_2-r_1)/2a$, r_1 being the electron-impurity distance, and r_2 the distance of the electron to the image impurity, located at $z=-a$. For the exciton problem, only the ground state is of interest; its energy is plotted in Fig. 1 (full line). Taking advantage of the guess that the image potential is small for the relevant physical situation, as discussed before, we evaluate its expectation value on the ground state by numerical integration. Apart from the factor $(\epsilon-1)/(\epsilon+1)$ in (1), the expectation value, measured in terms of the effective Rydberg, is a universal function of a/a_B, which is tabulated in Table I. The impurity ground-state energy in the case of GaAs, calculated including the image potential, is plotted in Fig. 1 (dashed line). The image-potential expectation value diverges as a tends to zero, due to the diverging repulsive interaction of the impurity with its image; otherwise, however, it is quite small. Hence the use of first-order perturbation theory for a larger than a_B is justified.

Our approach can be considered variational; in fact, we calculate the expectation value of the total Hamiltonian, including the image potential, on the exact eigenstates of the zero-order Hamiltonian, without the image potential. Our results can be compared with those of the variational approach of Shen *et al.*,[11] who used exponential trial wave functions (times a linear term in z_e, which ensures the fulfillment of the "no-escape" boundary condition at the surface) for both Hamiltonians. The results of Shen *et al.*[11] are compared with those of Satpathy in Fig. 2(a), for the case where the image potential is neglected. The image potential is included in the curves of Fig. 2(b), except the repulsive interaction of the impurity with is image, namely, the constant $(e^2/4\epsilon a)[(\epsilon-1)/(\epsilon+1)]$, which was not included by Shen *et al.* We find that our

TABLE I. Expectation value of the image potential as a function of the impurity distance from the surface. The multiplicative factor $(\epsilon-1)/(\epsilon+1)$ Ry* in (1) is not included here.

a/a_B	$\langle V_{\rm Im}\rangle$/Ry*
0.0	∞
0.1	4.682
0.2	2.176
0.3	1.336
0.4	0.910
0.5	0.652
0.6	0.480
0.7	0.360
0.8	0.276
0.9	0.218
1.0	0.176
1.1	0.144
1.2	0.124
1.3	0.106
1.4	0.092
1.5	0.080
1.6	0.072
1.7	0.064
1.8	0.058
1.9	0.052
2.0	0.044
2.5	0.020
∞	0.000

ground-state energy is lower than that of Ref. 11 for $a > a_B$. This is of course a consequence of using a better trial wave function than that of Shen *et al.* The effect of the image potential, already small, agrees in the two calculations within 10%; the discrepancy is smaller than 0.03 effective Rydbergs for $a > a_B$. This is estimated to be the precision of our calculation in this range, which is relevant for the exciton problem.

III. EXCITON

In this section we will apply the results obtained for the near-surface impurity to the exciton problem. The effective-mass Schrödinger equation is in this case

$$\left[-\frac{\hbar^2}{2\mu}\nabla^2_{\vec{r}}-\frac{\hbar^2}{2M}\frac{\partial^2}{\partial Z^2}-\frac{e^2}{\epsilon r}+V_{\rm Im}(\vec{\rho}_e-\vec{\rho}_h;z_e,z_h)\right]$$

$$\times\Psi(\vec{\rho}_e-\vec{\rho}_h;z_e,z_h)=E\Psi(\vec{\rho}_e-\vec{\rho}_h;z_e,z_h)\ . \quad (4)$$

We separate adiabatically the center-of-mass slow motion along Z from the fast e-h relative motion along z and $\vec{\rho}$. The latter is described by a Schrödinger equation similar to (2), where m_e is replaced by the reduced mass μ, and $\vec{r}_e$ by $(\vec{\rho},z)$. Because of the no-escape boundary condition, the relative wave function must vanish at $z=-MZ/m_h$ and at $z=MZ/m_e$. Since the latter quantity is much larger than the exciton radius (for Z of the order of a_B), the vanishing of the wave function is trivially ensured there; we can limit ourselves to the first boundary condition, which makes the problem equivalent to that of an impurity at $a=MZ/m_h$. This approach has been already used with excellent results in Ref. 7, where the image potential was neglected. Here we will extend it in a quite straightforward way to account for the image potential.

As in Ref. 7, the exciton center-of-mass motion in the potential shown in Fig. 1 is solved numerically. Then, as in Ref. 9, the exciton wave function at $(\vec{\rho},z)=0$, which is important for determining optical properties, is approximated by a model analytical wave function involving a dead layer d below the surface, where the exciton is not present at all, and a transition layer, of depth $1/P$, where the probability of finding the exciton continuously increases from zero to the bulk value:

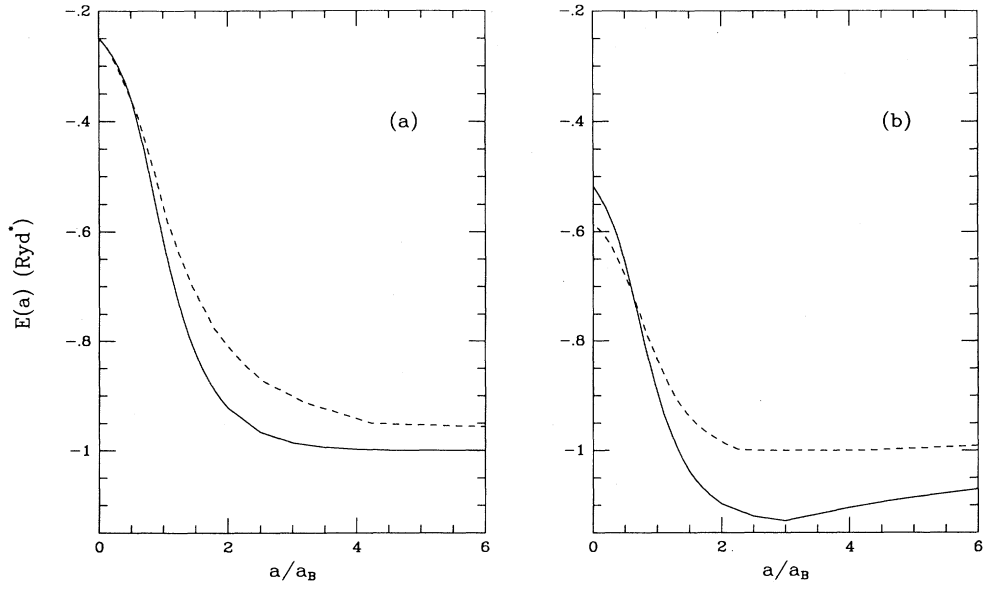

FIG. 2. (a) Ground-state energy of a hydrogenic impurity as a function of the distance a from the surface. Image-potential effects are not included. Solid line: Satpathy's exact calculation (Ref. 8). Dashed line: variational approach of Shen *et al.* (Ref. 11). (b) As in (a), including the interaction of the electron with its image and with that of the impurity, but not the interaction of the impurity with its image. Solid line: our results, where the image potential is accounted for by first-order perturbation theory. Dashed line: variational approach of Shen *et al.* (Ref. 11).

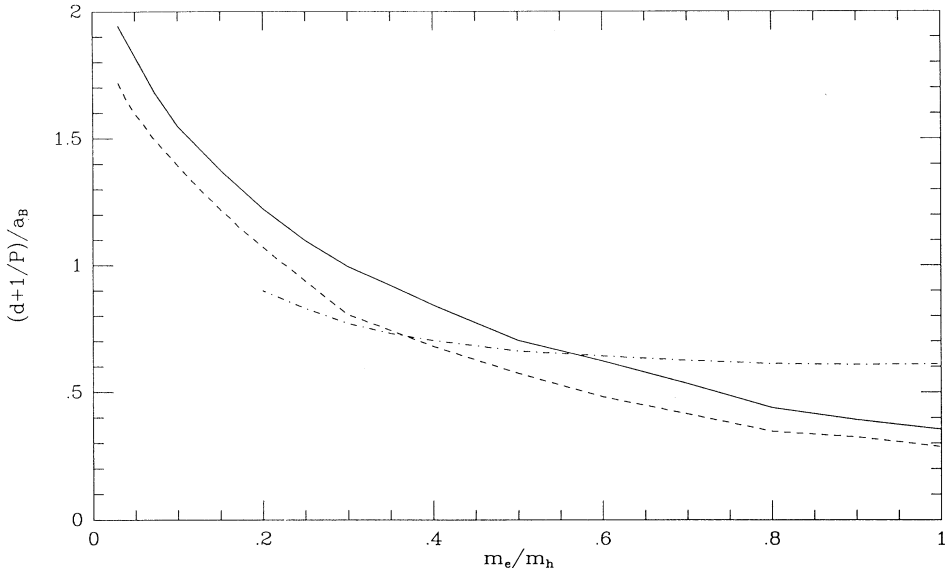

FIG. 3. Sum of the dead-layer depth d and of the transition layer depth $1/P$ of the analytical wave function (5) without the image potential (dashed line) and with the image potential (full line). Dot-dashed line: $1/P$ of the numerical nonadiabatic wave function of Ref. 7 (from Fig. 3 of Ref. 7).

$$\Psi(0,Z)=\begin{cases} 0 \quad \text{if } 0\le Z\le d \\ \dfrac{1}{\sqrt{2\pi}}[e^{-iK_Z(Z-d)}+Ae^{iK_Z(Z-d)} \\ -(1+A)e^{-P(Z-d)}]\phi_{100}(0) \quad \text{if } Z>d \end{cases}$$

with

$$A=-\frac{P-iK_Z}{P+iK_Z}\ . \tag{5}$$

d and P are chosen in order to reproduce at best the numerical $\Psi(0,Z)$. The procedure is the same as in Ref. 9, with the difference that here we consider both cases, with and without the image potential. The quality of the fit is as in Ref. 9.

IV. RESULTS

The main limitation of the present approach arises from the adiabatic approximation, which is valid for small values of μ/M. Although for $m_e/m_h=1$ it is already $\mu/M=1/4$, it is clear that the adiabatic approximation cannot be used in the whole range of m_e/m_h values with the high accuracy needed to determine the dead layer. For values of m_e/m_h of the order of unity, a numerical solution of the exciton Schrödinger equation, not relying on the adiabatic approximation, has been carried out.[1,7] For $m_e/m_h=0.3$ the wave function obtained within the latter approach perfectly agree with the adiabatic ones.[7] Therefore we hope that the adiabatic approach is valid also for values of m_e/m_h larger than 0.3. In order to assess this point, we plot in Fig. 3 the sum of the dead-layer plus transition-layer depths as determined

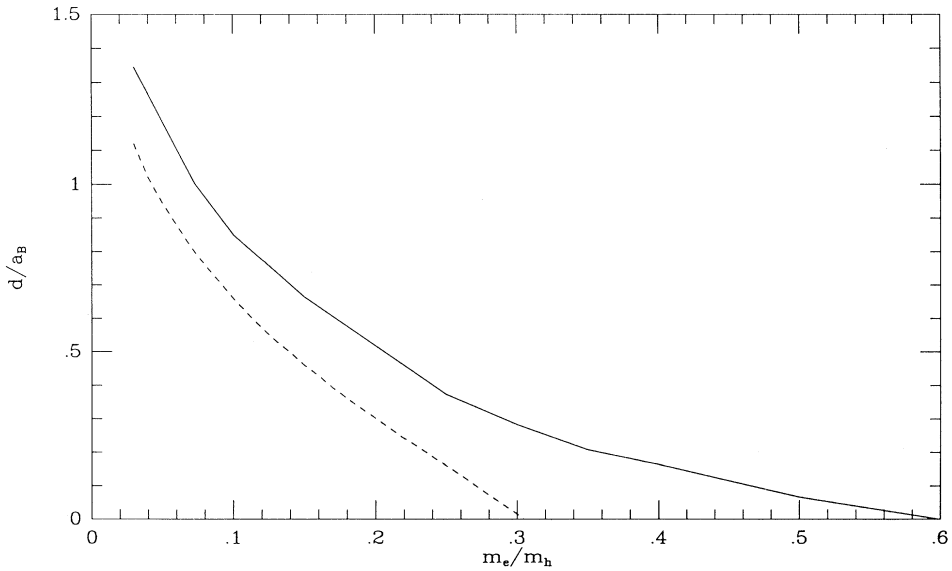

FIG. 4. Exciton dead-layer depth d of the analytical wave function (5) as a function of the mass ratio m_e/m_h, without the image potential (dashed line) and with the image potential (full line).

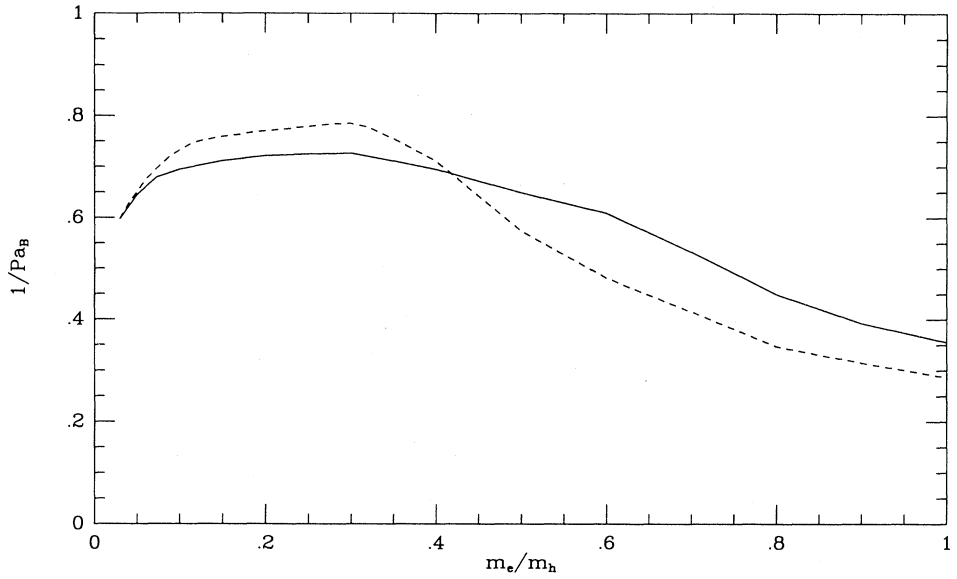

FIG. 5. Transition-layer depth $1/P$ of the analytical wave function (5) as a function of the mass ratio m_e/m_h, with (full line) and without (dashed line) the image potential.

by the adiabatic approach (without the image potential, dashed line) together with the transition-layer depth of the numerical wave functions (dot-dashed line). $(d+1/P$ is the right quantity to use for the sake of comparison, because the numerical wave functions have been described only in terms of the transition layer, since the dead layer was not necessary in the range of higher m_e/m_h values.) From Fig. 3 it is evident that there is a very good agreement for m_e/m_h between 0.3 and 0.4, and also that the adiabatic approximation is valid within 10% up to $m_e/m_h=0.5$. Moreover, since the image potential effect is small (see Fig. 3, full line), we would like to use the present approach, based on the adiabatic approximation, also for values of m_e/m_h larger than 0.5 *only to determine the image-potential effect.* We describe now the results obtained including the image potential, using the value of the dielectric constant of GaAs ($\epsilon=12.6$). In Fig. 4 the dead-layer depth d, with and without the image-potential effect, is shown. The effect of the image potential is to increase d by a quantity varying from $0.2a_B$ (for small m_e/m_h) to $0.3a_B$ (at $m_e/m_h=0.3$), to zero (for m_e/m_h larger than 0.6). The most evident effect is to extend the range where d is nonvanishing, from $m_e/m_h<0.3$, to $m_e/m_h<0.6$. The transition-layer depth, with and without the image potential, is plotted in Fig. 5. Image-potential effects decrease (for $m_e/m_h<0.4$) or increase (for $m_e/m_h>0.4$) $1/P$ by less than $0.1a_B$. Its effect on the sum $d+1/P$ turns out to be quite small, as is shown in Fig. 3.

Finally, in Fig. 6 we try to give as complete a picture as possible of the exciton behavior near the surface for all values of m_e/m_h. For $m_e/m_h<0.3$, we plot $(d+1/P)$

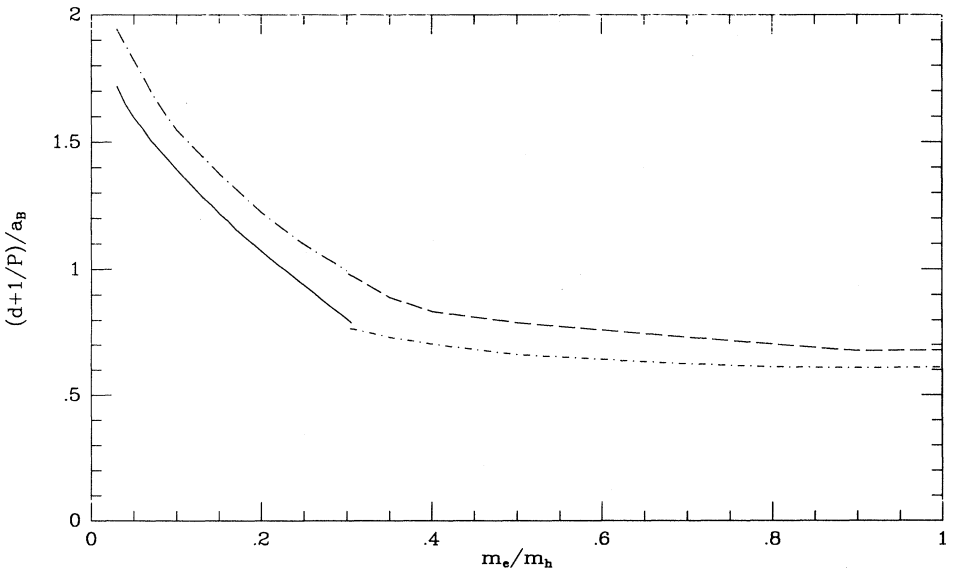

FIG. 6. For $m_e/m_h<0.3$, $d+1/P$ without the image potential (full line) and with the image potential (dot-long-dashed line). For $m_e/m_h>0.3$, $1/P$ of the numerical nonadiabatic wave function of Ref. 7 not including the image potential (dot-dashed line) and with the effect of the image potential summed over (long-dashed line).

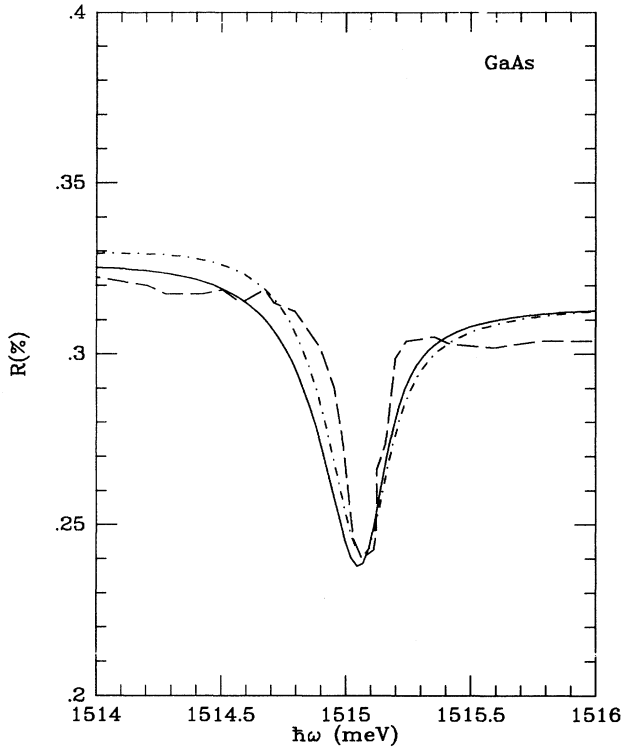

FIG. 7. Normal-incidence reflectance of GaAs. Experiment from Ref. 16, dashed line. Our calculation, full line. Excitonic parameters used in the calculation: $\hbar\omega_0=1.515$ eV, $4\pi\alpha_h=0.22\times10^{-2}$, $\epsilon_0=12.6$, $M=0.79$ m, $m_e/m_h=0.064$, $d=158.4$ Å, $1/P=99$ Å, and $\Gamma=0.095$ meV. Dot-dashed line: calculation from Ref. 9, which neglects the image potential, with $d=125.8$ Å, $1/P=102$ Å.

as determined according to the present adiabatic approach with and without the image potential. For $m_e/m_h>0.3$, we report $1/P$ of the numerical wave function determined without the image potential, and sum to it the effect of the image potential as determined within the adiabatic approach (long-dashed line), namely, the difference of the two curves in Fig. 3. It can be seen that the final effect of the image potential is quite small; that is, it increases the sum of dead- and transition-layer depths by at most $0.2a_B$.

One expects that such a small increase of the dead- and transition-layer depths has negligible effects on optical spectra, since it is well known that large changes (of the order of a_B) of the dead layer determine small (of the order of 5%) changes of the reflectance intensity.[12,13] We show that this is indeed the case in Fig. 7, where the reflectance of the heavy exciton in GaAs is calculated as in Ref. 9. The full line, embodying the image potential, is very similar to that calculated in Ref. 9 without the image potential (dot-dashed line). In particular, the steplike increase of reflectance on the high-frequency side of the resonance appearing in the experimental spectrum (see Fig. 7) is not obtained in our calculation, even including the image potential. Therefore the latter cannot explain this slight discrepancy between theory and experiment in exciton reflectivity occurring in GaAs and—to a lesser extent—in InP.[9]

V. CONCLUSIONS

We have calculated the effect of the image potential on excitons in a semi-infinite semiconductor. Such an effect is shown to be quite small: it increases the dead- and transition-layer depth sum by less than $0.2a_B$, in agreement with previous estimates. The reason for this is that the exciton repulsion from the surface, which is its main effect, is already accounted for by the "no-escape" boundary condition; as a consequence, the exciton cannot come too close to the surface, where the image potential is important. At distances from the surface larger than the exciton radius, the exciton is seen from the surface mainly as a neutral point particle, inducing a small image potential.

As a consequence of the small effect of the image potential on the dead layer, its effect on reflectance spectra is also small. In particular, the image potential cannot explain the slight discrepancy between theory and experiment in exciton reflectivity occurring in GaAs and—to a lesser extent—in InP on the high-frequency side of the resonance. Such discrepancies must have an extrinsic origin, related to residual built-in electric fields at the surface and/or to the presence of surface states: both effects invalidate the simple infinite-barrier picture of the surface assumed in this and in most other papers about exciton reflectance.

Finally, we would like to emphasize that this work is the conclusion of a long effort aimed at finding exciton wave functions in a semi-infinite semiconductor.[14,1,12,7,13,9] A coherent picture has emerged, with the simultaneous occurrence of a dead layer (for $m_e/m_h<0.6$) and of a transition layer, whose depths depend on the e-h mass ratio. Their sum ranges from $2a_B$ for small m_e/m_h, in agreement with early experimental estimates,[15] to less than a_B for m_e/m_h larger than 0.3. The latter finding is also in agreement with several types of optical experiments in CdS and similar materials.[13] The slight discrepancies remaining in the cases of GaAs and InP must be due to extrinsic reasons.

[1]A. D'Andrea and R. Del Sole, Phys. Rev. B **25**, 3174 (1982).
[2]J. J. Hopfield and D. G. Thomas, Phys. Rev. **132**, 563 (1963).
[3]See, for instance, P. Halevi, in *Spatial Dispersion in Solids and Plasmas,* edited by P. Halevi (North-Holland, Amsterdam, 1992), p. 339.
[4]S. Sakoda, J. Phys. Soc. Jpn. **40**, 152 (1976).
[5]I. Balslev, Phys. Status Solidi B **88**, 155 (1978).
[6]I. Balslev, Phys. Rev. B **23**, 3977 (1981).
[7]A. D'Andrea and R. Del Sole, Phys. Rev. B **32**, 2337 (1985).
[8]S. Satpathy, Phys. Rev. B **28**, 4585 (1983).
[9]D. Viri, R. Del Sole, and A. D'Andrea, Phys. Rev. B **48**, 9110 (1993).

[10]D. B. Tran Thoai, R. Zimmermann, M. Grundmann, and D. Bimberg, Phys. Rev. B **42**, 5906 (1990).
[11]Z. J. Shen, X. Z. Yuan, B. C. Yang, and Y. Shen, Phys. Rev. B **48**, 1977 (1993).
[12]A. D'Andrea and R. Del Sole, Phys. Rev. B **29**, 4782 (1984).
[13]A. D'Andrea and R. Del Sole, Phys. Rev. B **38**, 1197 (1988).
[14]A. D'Andrea and R. Del Sole, Solid State Commun. **30**, 145 (1979).
[15]F. Evangelisti, A. Frova, and F. Patella, Phys. Rev. B **10**, 4253 (1974); F. Evangelisti, J. U. Fischbach, and A. Frova, *ibid.* **9**, 1516 (1974).
[16]L. Schultheis and I. Balslev, Phys. Rev. B **28**, 2292 (1983).